Molecular Pharmacology Fast Forward. Published on June 25, 2012 as doi:10.1124/mol.112.079962
This article has not been copyedited and formatted. The final version may differ from this version.

Contribution of Subunits to *C. elegans* Levamisole-Sensitive Nicotinic Receptor Function

Guillermina Hernando, Ignacio Bergé, Diego Rayes and Cecilia Bouzat

Instituto de Investigaciones Bioquímicas de Bahia Blanca- Universidad Nacional del Sur/CONICET-8000 Bahia Blanca-Argentina

Molecular Pharmacology Fast Forward. Published on June 25, 2012 as DOI: 10.1124/mol.112.079962
This article has not been copyedited and formatted. The final version may differ from this version.

Running Title: *C. elegans* muscle AChRs

Corresponding author: Cecilia Bouzat. Instituto de Investigaciones Bioquímicas de Bahía Blanca. Camino La Carrindanga Km 7. 8000 Bahia Blanca. Argentina. E-mail: inbouzat@criba.edu.ar. Telephone: 54-291-4861201- FAX: 54-291-4861200

Number of text pages: 39

Number of tables: 1

Number of Figures: 7

Number of References: 49

Number of words in the *Abstract:* 206

Number of words in the *Introduction*: 778

Number of words in the *Discussion:* 1498

Abbreviations: AChR, nicotinic acetylcholine receptor; ACh, acetylcholine; L-AChR, levamisole-sensitive AChR; N-AChR, nicotine-sensitive AChR; Popen, probability of channel opening.

Molecular Pharmacology Fast Forward. Published on June 25, 2012 as DOI: 10.1124/mol.112.079962
This article has not been copyedited and formatted. The final version may differ from this version.

Abstract

C. elegans muscle contains seven different nicotinic receptor (AChR) subunits, five of which have been shown to be components of adult levamisole-sensitive AChRs (L-AChRs). To elucidate the reason for such subunit diversity we explore their functional roles in larva 1 (L1) muscle cells. Single-channel and macroscopic current recordings reveal that the α-type LEV-8 subunit is a component of native L1 L-AChRs but behaves as a non essential subunit. It plays a key role in maintaining a low rate and extent of desensitization of L-AChRs. In the absence of the α-type ACR-8 subunit L-AChR channel properties are not modified, thus indicating that ACR-8 is not a component of L1 L-AChRs. Together with our previous findings, this study reveals that L1 muscle cells express a main L-AChR type composed of five different subunits: UNC-38, UNC-63, UNC-29, LEV-1 and LEV-8. Analysis of a double *lev-8/acr-8* null mutant, which shows uncoordinated and levamisole-resistant phenotype, reveals that ACR-8 can replace LEV-8 in its absence, thus attributing a functional role to this subunit. Docking into homology modeled L-AChRs proposes that ACh forms the typical cation-π interaction, suggests why levamisole is less efficacious than ACh, and shows that ACR-8 can form activatable binding-sites, thus opening doors for elucidating subunit arrangement and anthelmintic selectivity.

Molecular Pharmacology Fast Forward. Published on June 25, 2012 as DOI: 10.1124/mol.112.079962
This article has not been copyedited and formatted. The final version may differ from this version.

Introduction

The nicotinic acetylcholine receptor (AChR) is a member of the Cys-loop receptor family, which mediates fast synaptic transmission in vertebrates and invertebrates. AChRs can assemble from five identical α-type subunits, forming homomeric receptors, such as vertebrate α7 or *Caenorhabditis elegans* ACR-16 (N-AChR), or from different α and non-α subunits, forming heteromeric receptors, such as vertebrate and *C. elegans* muscle L-AChRs (Taly et al., 2009; Bouzat, 2012). AChR contains a large extracellular domain, which carries the agonist binding sites, and a transmembrane region that forms the ion pore (Unwin, 2005). The agonist binding sites are formed at interfaces between subunits (Brejc et al., 2001), with the principal face formed by residues of an α-type subunit and the complementary face, by residues of the adjacent subunit (α or non-α). Key residues of the principal face are grouped in regions called Loop A (W86 and Y93), Loop B (W149 and G153), and Loop C (Y190, C192, C193 and Y198) (numbering from *Torpedo* AChR). At the complementary face, key residues are clustered in Loop D (W55), E (L109, Y111, Y117 and L119) and F (D174 and E176) (Brejc et al., 2001; Bartos et al., 2009a; Bouzat, 2012).

Nematode muscle AChRs are of clinical importance since they are targets of anthelmintic drugs. Nematode parasites cause substantial mortality and morbidity in human population and losses in livestock and domestic animals. The free-living nematode *C. elegans* is a valuable tool for the study of anthelmintic targets because it shares physiological and pharmacological characteristics with parasitic nematodes and it is sensitive to most anthelmintic drugs (Jones et al., 2005; Neveu et al., 2010). *C. elegans* has also emerged as a useful model organism for studying human neuromuscular diseases and for drug testing (Jones et al., 2005, 2011).

Genetic analyses demonstrated the expression of at least 29 AChR subunits in *C. elegans* (Brown et al., 2006; Rand, 2007). The way that subunits co-assemble into pentameric receptors is still unknown. Two different types of AChRs, N-AChR and L-AChR, are present at the neuromuscular junction (Richmond and Jorgensen, 1999). The N-AChR, which is sensitive to

nicotine, is a homopentamer formed by ACR-16 (Touroutine et al., 2005; Francis et al., 2005). The L-AChR is the target of nematocide agents, such as levamisole and pyrantel. By acting as potent agonists of nematode AChRs and without being rapidly degraded, these drugs produce body-wall muscle hypercontraction, paralysis, and ultimately death of *C. elegans* and parasitic nematodes. These anthelmintics are highly selective for nematode AChRs whereas they are very low-efficacy agonists of vertebrate muscle AChRs (Rayes et al., 2004).

Analysis of *C. elegans* levamisole-resistant mutant strains has shown that the α-type UNC-63, UNC-38, and LEV-8 subunits and the non-α UNC-29 and LEV-1 subunits are components of the adult L-AChR (Fleming et al., 1997; Culetto et al., 2004; Towers et al., 2005; Almedom et al., 2009). Boulin *et al.* (2008) reconstituted functional L-AChRs in *Xenopus laevis* oocytes by co-expressing the five different L-AChR subunits together with three ancillary proteins. ACR-8, an α-type subunit highly homologous to LEV-8 (Mongan et al., 1998), is also present in muscle but its function remains unclear (Touroutine et al., 2005; Gottschalk et al., 2005).

The native composition of L-AChR(s) in larval muscle cells remains unknown. It could be possible that the subunit expression pattern changes during development as occurs in human (Hall and Sanes, 1993), which, in turn, could be translated into different drug sensitivity between larval and adult stages (Lewis et al., 1980). Thus, deciphering potential differences in the molecular anthelmintic targets between both developmental stages is of considerable interest, not only from a physiological point of view, but also for drug development.

We have previously shown that whereas single L-AChR channel activity is readily detected in Larva 1 (L1) muscle cells from wild-type strain it is not detected in cells from *unc-29*, *unc-63* or *unc-38* null mutants, indicating that these subunits co-assemble into a single functional L-AChR (Rayes et al., 2007). Functional L-AChRs are also detected in a *lev-1* mutant strain, indicating that this subunit is not essential (Rayes et al., 2007). Therefore, in order to decipher the composition of larval L-AChRs, we here explore single-channel and macroscopic current properties of L1 muscle

receptors from *lev-8* and *acr-8* null mutants (Towers et al., 2005; Mongan et al., 2002) as well as from a double null mutant, thus fully covering the analysis of the contribution of all muscle subunits to L-AChR function. We also determined the contribution of L- and N-AChRs to ACh-elicited muscle responses at L1. The experimentally obtained information was combined with molecular docking studies in homology modeled L-AChRs to provide testable hypothesis about how subunits assemble into L-AChRs and how anthelmintic agents interact with this receptor.

Molecular Pharmacology Fast Forward. Published on June 25, 2012 as DOI: 10.1124/mol.112.079962
This article has not been copyedited and formatted. The final version may differ from this version.

Materials and Methods

Isolation and culture of C. elegans muscle cells: Nematode strains (N2 Bristol wild-type; PD4251: *ccIs4251;dpy-20(e1282)*; ZZ15: *lev-8(x15);* VC1041:*lev-8(ok1519)X;* RB1195: *acr-8(ok1240)*; RB918: *acr-16(ok789);* CB1072: *unc-29(e1072*)), were obtained from the *Caenorhabditis* Genetic Center, which is funded by the NIH National Center for Research Resources (NCRR). When necessary, the strains were backcrossed at least four times. Nematodes were maintained at 18-25 °C using standard culture methods. Embryonic cells were isolated and cultured at 22 °C (Christensen et al., 2002; Rayes et al., 2007; Almedom et al., 2009). Complete differentiation to the cell types that comprise the newly hatched larva 1 (L1) was observed within 24 h and muscle cells were easily identifiable due to their spindle-shaped morphology (Christensen et al., 2002). Electrophysiology experiments were performed 2-6 days after cell isolation.

Patch-clamp recordings: Single-channel currents were recorded in the cell-attached configuration essentially as described previously (Rayes et al., 2007). The bath and pipette solutions contained 142 mM KCl, 5.4 mM NaCl, 1.8 mM $CaCl_2$, 1.7 mM $MgCl_2$, and 10 mM HEPES (pH 7.4). Single-channel currents were recorded using an Axopatch 200 B patch-clamp amplifier (Molecular Devices Inc., CA, USA), digitized at 5 μs intervals with the PCI-611E interface (National Instruments, Austin, TX), recorded using the program Acquire (HEKA Instruments Inc., NY, USA), and detected by the half-amplitude threshold criterion using the program TAC 4.0.10 (Bruxton Corporation, Seattle, WA, USA) at a final bandwidth of 9 kHz. Open and closed time histograms were plotted using a logarithmic abscissa and a square root ordinate and fitted to the sum of exponentials by maximum likelihood using the program TACFit (Bruxton Corporation). Single-channel activity from wild-type strains (N2 (Bristol) and myo-3::GFP PD4251 (Fire et al., 1998)) has been previously characterized in Rayes et al. (2007) and does not differ significantly from the one in this study.

Molecular Pharmacology Fast Forward. Published on June 25, 2012 as DOI: 10.1124/mol.112.079962
This article has not been copyedited and formatted. The final version may differ from this version.

Bursts and clusters of channel openings were identified as a series of closely separated openings preceded and followed by closings longer than a critical duration (τ_c), which was taken as the point of intersection of components in the closed time histogram (Gumilar et al., 2003; Corradi et al., 2009). For bursts, τ_c was defined by the point of intersection of the briefest duration component and the succeeding one (typically 250-400 μs), and for clusters, between the slowest closed component and the previous one (typically 0.4-1.0 s for 100 μM ACh and 0.25-0.60 s for 300 μM ACh). Burst and cluster durations were determined from the longest duration component of open time histograms with τ_c set to the corresponding value, and therefore openings separated by closings briefer than this time constitute a burst or a cluster. Open probability within clusters (P_{open}) was estimated for each recording by the mean fraction of time that the channel is open within a cluster as follows: P_{open}= (number of bursts per cluster x mean burst duration)/ mean cluster duration. Macroscopic currents elicited by a pulse of agonist were recorded in the whole-cell configuration at 22ºC, filtered at 5 kHz, and digitized at 20 kHz (Gumilar et al., 2003; Corradi et al., 2009). The pipette solution contained 134 mM KCl, 10 mM EGTA, 1 mM $MgCl_2$, and 10 mM HEPES (pH 7.3). The extracellular solution (ECS) contained 140 mM NaCl, 3 mM $CaCl_2$, 5 mM KCl, 5 mM $MgCl_2$, 11 mM glucose, 5 mM HEPES (pH 7.4). Data analysis was performed using the IgorPro software (WaveMetrics Inc., Lake Oswego, OR, USA). Each current trace is the ensemble average of 3-5 individual traces from the same cell, which were aligned at the point where the current reached 50% of the peak current. The rise time was determined from the time between 20% and 80% of the peak current (t_{20-80}). Currents were fitted by a double-exponential function: $I_{(t)}=I_1(\exp(-t/\tau_1))+I_2(\exp(-t/\tau_2)) + I_\infty$, where I_∞ is the steady state current and τ_1 and τ_2 are the decay time constants.

Homology modeling and molecular docking: Homology models of the extracellular domain of the whole L-AChR or of two adjacent subunits were created using the structure of the nicotine-bound *Lymnaea stagnalis* Acetylcholine Binding Protein (AChBP, PDB 1UW6) as template. The amino

Molecular Pharmacology Fast Forward. Published on June 25, 2012 as DOI: 10.1124/mol.112.079962
This article has not been copyedited and formatted. The final version may differ from this version.

acid sequences were aligned using CLUSTALW and modeling was performed using MODELLER 9 v.7 (Sali et al., 1995). Loop F is not well resolved in the AChBP structure (Brejc et al., 2001; Reeves et al., 2003). Moreover, Loop F of α-type *C. elegans* subunits (UNC-63, UNC-38, LEV-8 and ACR-8) is between 16 and 27 amino acids longer than that of AChBP. We have therefore not included this loop in our analysis because it cannot be modeled reliably. We tested eight different subunit interfaces derived from four different pentameric arrangements and three additional interfaces in which ACR-8 replaces LEV-8 as the principal face. Ten models were generated for each interface, and the one with the lowest energy and the smallest percentage of amino acids in the disallowed region of the Ramachandran plot was selected for docking studies. No differences were found in the docking results if the template binding-site interface was obtained from modeling the whole receptor or two adjacent subunits. Protonated levamisole was constructed with Discovery Studio Visualizer 2.5 (Accelrys Software Inc.). ACh and levamisole were docked separately using AutoDock 4.3 (Morris et al., 1998) into the ligand binding site, which was defined as being within 20 Å of W149. A hundred genetic algorithm runs were performed for each condition. Clustering of the results was done with AutoDock based on a RMSD cut-off of 2.0 Å. Docking results were corroborated in 2-4 different procedures.

Measurements of motility and levamisole resistance: Thrashing assays, used to measure worm motility, were performed as described (Jones et al., 2011). A single thrash was defined as a change in the direction of bending at the mid body. All assays were blind and carried out at 21 °C. Levamisole resistance was determined on agar plates containing 0.2 mM levamisole at room temperature. Body paralysis was followed by visual inspection every 15 minutes and was defined as the lack of body movement in response to prodding. As previously reported for the *lev-8* null mutant (Lewis et al., 1980; Almedom et al., 2009), we observed that under the present conditions levamisole leads to paralysis of the body, which was the evaluated parameter, but does not affect significantly the head movement.

Molecular Pharmacology Fast Forward. Published on June 25, 2012 as DOI: 10.1124/mol.112.079962
This article has not been copyedited and formatted. The final version may differ from this version.

Statistics: Experimental data are shown as mean ± SD. Statistical comparisons were done using the Student's *t* test or One-way ANOVA with Bonferroni's multiple comparison post test. A level of $p < 0.05$ was considered significant.

Molecular Pharmacology Fast Forward. Published on June 25, 2012 as DOI: 10.1124/mol.112.079962
This article has not been copyedited and formatted. The final version may differ from this version.

Results

Functional changes of L-AChRs lacking LEV-8.

We first examined how the absence of the LEV-8 subunit affects worm behavior by measuring motility and susceptibility to the anthelmintic levamisole. *lev-8* null mutants show no significant changes in the thrashing rate in M9 liquid medium with respect to wild-type (182.4 ± 22.1 and 175.6 ± 24.1 thrashes/ min for wild-type and *lev-8* null mutant, respectively, $p > 0.5$, Fig. 1A). However, they show partial resistance to levamisole, in agreement with previous reports (Lewis et al., 1980; Towers et al., 2005) (Fig. 1A).

We next determined the contribution of LEV-8 to L-AChR function by measuring single-channel currents in Larva 1 (L1) muscle cells derived from a *lev-8* null mutant strain (*lev-8(x15)*). L-AChR channels activated by ACh or levamisole are detected in cell-attached patches, indicating that LEV-8 is not essential for expression of functional L-AChRs at this developmental stage (Figs. 1B and 2). In contrast, channel activity is not detected in null mutants of UNC-63, UNC-38 or UNC-29 subunits (Rayes et al., 2007). The relationship between the amplitude of openings and membrane potential reveals that L-AChRs lacking LEV-8 exhibits an inward conductance of 35 ± 0.9 pS, similar to that of wild-type L-AChRs (35 ± 1.2 pS, Fig. 2).

Single-channel activity at low ACh concentration (0.1–1 μM) occurs as isolated openings or as short bursts of openings in quick succession (Figs. 1 and 3 and Rayes et al., 2007). Open time histograms of L-AChRs lacking LEV-8 (0.1-1 μM ACh) are fitted by the sum of two exponential components whose mean durations are 2-fold more prolonged than those of wild-type L-AChRs (Table 1, Fig. 1). Mean burst duration of L-AChRs from *lev-8(x15)* (1.51 ± 0.38 ms) is more prolonged than that from wild-type (0.65 ± 0.05 ms, Student's *t*-test $p<0.005$). In the presence of 1 μM levamisole, open time histograms are fitted by two components and the duration of the slowest one is ~3-fold more prolonged than that of wild-type L-AChRs (Table 1, Fig. 1).

Molecular Pharmacology Fast Forward. Published on June 25, 2012 as DOI: 10.1124/mol.112.079962
This article has not been copyedited and formatted. The final version may differ from this version.

We next analyzed L-AChR channels from *lev-8(x15)* at a range of agonist concentration (Fig. 3). The duration of the slowest open component decreases with ACh and levamisole concentration, indicating agonist-induced open-channel block (Supplemental Figure 1).

Closed time distributions of L-AChRs from the mutant strain are well described by the sum of three or four components (Fig. 3). The briefest closed component (~60 μs) does not change but its relative area systematically increases with ACh concentration (0.20 ± 0.07 at 1 μM ACh and 0.57 ± 0.075 at 100 μM). This is due to the fact that brief closings arising from open-channel block superimpose in the histogram with brief closings that correspond to the activation process (Rayes et al., 2007). The increase in the area of the briefest closed component as a function of agonist is not so clear for levamisole, which could be indicative of slow open-channel block.

The mean duration of the main closed component of ACh-activated channels does not show significant differences between wild-type and mutant L-AChRs. In parallel with the increase in the frequency of opening events, the duration of the closed component decreases as a function of concentration in both L-AChRs (Fig. 3). The mean values of this closed component for wild-type and *lev-8(x15)* are: 1200 ± 460 ms (n= 4) and 1200 ± 590 ms (n= 6) at 0.5 μM ACh; 460 ± 320 ms (n=9) and 430 ± 190 ms (n=7) at 1 μM ACh; 15 ± 5 ms (n=3) and 28 ± 22 ms (n=4) at 50 μM ACh; 18 ± 10 ms (n=8) and 26 ± 7 ms (n=5) at 100 μM ACh; 10 ± 4 ms (n=4) and 7 ± 1 ms (n=4) at 300 μM ACh, respectively.

For wild-type L-AChRs, the duration of the main closed component is briefer in the presence of 1 μM levamisole (100 ± 70 ms, n=6) than in the presence of 1 μM ACh, indicating that levamisole is a potent agonist. However, in L-AChR lacking LEV-8 it is more prolonged in the presence of 1 μM levamisole (1240 ± 380 ms, n=5) than 1 μM ACh. This finding indicates that the mutant is less sensitive to the anthelmintic drug in agreement with our results from the paralysis assay (Fig. 1).

Molecular Pharmacology Fast Forward. Published on June 25, 2012 as DOI: 10.1124/mol.112.079962
This article has not been copyedited and formatted. The final version may differ from this version.

Single-channel activity of L-AChRs lacking LEV-8 decreases markedly with time and occurs in clusters.

The activation profile of L-AChR lacking LEV-8 exhibits remarkable differences compared to that of wild-type strain. The differences are clearly distinguished in recordings performed at high agonist concentrations. A dramatic decrease in single-channel activity during the course of the recording and the appearance of clusters of opening events are observed in the *lev-8* null mutant but not in the wild-type (Fig. 4).

In order to quantify the decrease of single-channel activity as a function of time, which was clearly detected from visual inspection of the recordings, we measured the number of opening events per minute during the first seven minutes for each single-channel recording (Fig. 4A). We only used recordings from cell-attached patches with rapidly formed seals. It is important to clarify that overlapping openings are very infrequent in our single-channel recordings, even during the first seconds after seal formation, and therefore they do not affect the frequency measurements. Also, there is no evidence of rundown in our cell-attached patches. Given that at 100 μM ACh flickering block is observed, we considered each burst as an opening event. Thus, a burst includes the brief closings arising from open-channel block.

For wild-type L-AChRs activated by 100 μM ACh the number of bursts during the first minute of recording is 1700 ± 830 (n=4) and remains constant during the course of the recording (Fig. 4A). In the *lev-8(x15)* mutant the frequency of bursts is similar to that of wild-type during the first minute (1500 ± 700 bursts/ min, n=4) but it dramatically decreases thereafter. This decrease is illustrated in Fig. 4A, which shows that the number of opening events at the first minute corresponds to ~55% (ACh) and ~70 % (levamisole) of the total events in the 7-min recording and that channel activity is negligible after the first four minutes, evidencing only sporadic episodes of activity. Since each plot shows the mean value of the frequency of opening events along the

Molecular Pharmacology Fast Forward. Published on June 25, 2012 as DOI: 10.1124/mol.112.079962
This article has not been copyedited and formatted. The final version may differ from this version.

recording for a given strain, the difference in open durations between strains does not affect the conclusion that channel activity decreases more rapidly in the mutant than in the wild-type.

In addition to the decrease with time, channel activity of L-AChR lacking LEV-8 occurs in well defined activation episodes or clusters, which are distinguished as periods of intense channel activity separated by prolonged quiescent periods lasting several seconds (Fig. 4). Each cluster begins with the transition of a single receptor from the desensitized to the open state and terminates by returning to the desensitized state (Salamone et al., 1999). This profile contrasts with that observed in wild-type *C. elegans* muscle cells, in which clusters cannot be distinguished (Fig. 4A). We determined the properties of ACh-activated clusters at 100 and 300 μM ACh (Fig. 4B). The mean cluster duration is longer at 100 μM ACh (5.2 ± 1.5 s, n= 5) than at 300 μM ACh (2 ± 1.1 s, n=4, $p<0.005$) whereas the mean number of openings per cluster is similar at both concentrations (125 ± 10 and 150 ± 8 for 100 and 300 μM ACh, respectively), and the probability of channel opening within a cluster (Popen) increases with ACh concentration (0.015 ± 0.004 at 100 μM and 0.033 ± 0.02 at 300 μM ACh, $p<0.005$). The reduction in cluster duration and the increase in Popen as a function of ACh concentration are consistent with desensitization originating from fully-liganded states (Dilger and Liu, 1992; Auerbach and Akk, 1998).

As expected, L-AChR channel activity from *lev-8(ok1519)* is identical to that from *lev-8(x15)* strain. In agreement with data obtained from *lev-8(x15)* strain, single L-AChR channel activity from *lev-8(ok1519)* mutant shows open components of 0.58 ± 0.12 ms (relative area 0.78 ± 0.06) and 1.11 ± 0.37 ms (0.22 ± 0.06) at 1 μM ACh and clusters at 100 μM ACh, and decreases markedly with time (Supplemental Fig. 2).

The appearance of clearly distinguishable clusters and the profound decrease of channel activity as a function of time strongly suggest enhanced desensitization of L-AChRs lacking LEV-8.

Molecular Pharmacology Fast Forward. Published on June 25, 2012 as DOI: 10.1124/mol.112.079962
This article has not been copyedited and formatted. The final version may differ from this version.

Macroscopic current recordings reveal increased rate and extent of desensitization of L-AChR lacking LEV-8.

The profound decrease in channel activity as a function of time could be due to slower recovery and/or enhanced rate of desensitization. To further analyze the role of LEV-8 in receptor desensitization, we recorded macroscopic responses from L1 muscle cells elicited by high ACh concentrations in the whole-cell configuration at -70 mV. In wild-type muscle cells, a pulse of 500 μM ACh elicits currents that reach a peak in about 20 ms (t_{20-80}= 16 ± 10 ms) and decay slowly in the continuous presence of ACh (Fig. 5A). The mean peak current (I_{peak}) is -76 ± 18 pA (n=10). Decays are fitted by a double exponential function (τ_{fast}= 90 ± 30 ms (relative area 0.40 ± 0.09) and τ_{slow}= 580 ± 90 ms (0.21 ± 0.08)). Under the sustained pulse of agonist, the current at steady state (I_{ss}) is not zero probably because of recovery of desensitized receptors. Thus, the ratio between the steady state and peak current (I_{ss}/I_{peak}= 0.32 ± 0.08) is indicative of the extent of desensitization. In muscle cells derived from *lev-8(x15)* mutants, 500 μM ACh elicits inward currents with similar peak amplitudes to those observed in wild-type cells (I_{peak}= -85 ± 29 pA, n=9, Fig. 5A and C, p>0.5), indicating that the expression level is not significantly affected. However, currents decay significantly faster. Decays are fitted by two components but the duration of these components are between 3- and 4-fold briefer than those of wild-type L-AChRs (τ_{fast}= 29 ± 10 ms (relative area 0.55 ± 0.18), and τ_{slow}= 130 ± 48 ms (0.25 ± 0.10)). Although increased decay rates may result from open-channel block, this can be discarded since no difference in the apparent dissociation constant for channel block between wild-type and mutant L-AChRs is observed (Supplemental Fig. 1). Also, the I_{ss}/I_{peak} ratio is 2-fold smaller (0.19 ± 0.12), indicating increased extent of desensitization. Thus, the analysis of macroscopic responses reveals that both the rate and the extent of desensitization are significantly enhanced in L-AChRs lacking LEV-8. Unfortunately, these cultured muscle cells are not technically suitable for paired pulse drug applications and therefore we could not measure the time of recovery from desensitization.

Molecular Pharmacology Fast Forward. Published on June 25, 2012 as DOI: 10.1124/mol.112.079962
This article has not been copyedited and formatted. The final version may differ from this version.

Interestingly, the rise time is 3-fold briefer in the mutant strain (t_{20-80}= 6 ± 4 ms p<0.0001), showing that the activation rate is slightly increased in the mutant L-AChR.

Contribution of N-AChRs to ACh-responses in L1 muscle cells

To quantify the contribution of N-AChRs to the ACh-response in L1 cells we first recorded currents in a strain lacking N-AChR (*acr-16(ok789)*) (Fig. 5B). The analysis of ACh-elicited currents shows that the mean amplitude (-72 ± 25 pA, n=11, Fig. 5C), the decay time constants (τ_{fast}= 70 ± 35 ms (relative area 0.41 ± 0.09), τ_{slow}= 290 ± 160 ms (0.27 ± 0.10)), the I_{ss}/I_{peak} ratio (0.26 ±0.05), and the rise time (t_{20-80}= 18 ± 10 ms) are indistinguishable from those recorded from the wild-type strain.

One-way ANOVA with Bonferroni's multiple comparison post test between wild-type, *lev-8(x15)* and *acr-16(ok789)* resulted in p>0.50 for I_{peak}, p<0.0001 for τ_{fast}, and p<0.0001 for t_{20-80}. No statistically significant differences in any parameter between wild-type and *acr-16(ok789)* were found in the post test (p>0.50). Thus, in L1 muscle cells the majority of the ACh-activated current arises from the activation of L-AChRs and not from N-AChRs.

To further determine the direct contribution of N-AChRs to macroscopic responses we next attempted to record currents from cultured cells from the *unc-29(e1072)* strain, which lacks the essential UNC-29 subunit (Fig. 5B). Macroscopic currents elicited by ACh were detected only in 25 % of the tested muscle cells whereas in N2 wild-type, *lev-8(x15)* or *acr-16(ok789)* mutants > 95 % of the tested muscle cells showed ACh-activated currents. Studies on *unc-29(e1072)* showed that peak currents are significantly smaller than wild-type currents (I_{peak}= -25 ± 8 pA, n=3, p<0.001, Fig. 5C), decays are 40-fold faster than those of wild-type and 10-fold faster than those of L-AChRs lacking LEV-8 (τ_{fast}= 2.8 ± 1 ms (relative area 0.70 ± 0.02) and τ_{slow}= 37 ± 12 ms (0.20 ± 0.02)), and the steady state current is insignificant (I_{ss}/I_{peak}= 0.07 ± 0.05), revealing full desensitization. We could not detect currents elicited by 500 µM nicotine in any strain (n 3, for each strain). This could

Molecular Pharmacology Fast Forward. Published on June 25, 2012 as DOI: 10.1124/mol.112.079962
This article has not been copyedited and formatted. The final version may differ from this version.

be due to the fact that, in addition to low N-AChR expression, nicotine-elicited currents may be of smaller amplitude than ACh-elicited currents, as shown in oocytes (Boulin et al., 2008).

Thus, the contribution of N-AChR to the total ACh-activated current is insignificant in L1 muscle cells.

Levamisole is a partial agonist of L-AChRs

To further characterize the pharmacology of the L-AChR we measured responses of L1 cells to levamisole. In wild-type and *lev-8(x15)* (Fig. 5A), and *acr-16(ok789)* peak currents elicited by high levamisole concentrations (500 μM) (Culetto et al., 2004; Francis et al., 2005) are between 35-45% of those elicited by ACh. This result indicates that despite being a potent agonist, levamisole does not produce the maximal response.

The lack of ACR-8 does not affect single L-AChR channel activity

We explored single-channel properties of L1 muscle L-AChRs from the *acr-8* null mutant strain *(acr-8(ok1240))*. Channel activity elicited by ACh or levamisole is indistinguishable from that of the wild-type strain (Fig. 1). The duration of the slowest open component for ACh and levamisole (Table 1), the conductance (35 ± 1 pS, Fig. 2), and the lack of clusters at high ACh concentration reveal no changes in channel properties with respect to channels from wild-type strains. We conclude that this subunit is not a component of the wild-type L-AChR contributing to the major single-channel activity elicited by ACh or levamisole. In agreement to this, motility and levamisole sensitivity of worms not expressing ACR-8 subunit are similar to those of wild-type worms (Fig. 1A).

Single-channel activity from the double LEV-8/ACR-8 mutant: ACR-8 replaces LEV-8 in its absence.

Molecular Pharmacology Fast Forward. Published on June 25, 2012 as DOI: 10.1124/mol.112.079962
This article has not been copyedited and formatted. The final version may differ from this version.

Because ACR-8 shows the highest degree of conservation with LEV-8 we hypothesized that it could replace LEV-8 in the *lev-8* null mutant. To test this hypothesis, we generated the double LEV-8/ACR-8 mutant (*lev-8(ok1519)*; *acr-8(ok1240)*, Fig. 1).

Single-channel activity of *lev-8(ok1519)*; *acr-8(ok1240)* double null mutant shows clear differences with respect to that of wild-type and *acr-8* or *lev-8* single null mutants. First, in the presence of ACh or levamisole (1-100 μM) the percentage of patches showing channel activity is significantly lower than that of wild-type and *lev-8(x15)* mutant (~25 % for the double mutant and ~75% for wild-type and single null mutant, Supplemental Fig. 3).

Open time histograms obtained from the active patches in the presence of 1 μM ACh reveal a single brief open component (Table 1, Fig. 1) instead of the two components detected in wild-type and *lev-8* or *acr-8* null mutants (Table 1). The inward conductance is 36 ± 1.2 pS, similar to that of wild-type L-AChRs (Fig. 2). As in the *lev-8* null mutant, clusters of openings are observed at 100 μM ACh but they are briefer than those of LEV-8 null mutant (470 ± 190 ms, 78 ± 24 events/cluster, n=6) (Supplemental Fig. 3). The number of opening events/ min measured for the first minute of recording in the presence of 1 μM levamisole is significantly lower than that of wild-type (469 ± 395 (n=6) and 53 ± 32 (n=5) events/ min for wild-type and *lev-8(ok1519)*; *acr-8(ok1240)*, respectively), indicating reduced sensitivity to levamisole.

Thus, the fact that single-channel activity in the double mutant differs significantly from that of single LEV-8 and ACR-8 null mutants unequivocally demonstrates that ACR-8 can be incorporated into the pentamer in the absence of LEV-8.

We hypothesized that such profound changes at the single-channel level would be translated into significant phenotypic changes. As expected, the double LEV-8/ACR-8 null mutant shows impaired locomotion, as determined by a significant decrease in the thrashing rate (7.4-fold with respect to the wild-type), and strong resistance to levamisole (Fig. 1A).

Molecular Pharmacology Fast Forward. Published on June 25, 2012 as DOI: 10.1124/mol.112.079962
This article has not been copyedited and formatted. The final version may differ from this version.

Molecular docking of ACh and levamisole into L-AChR binding-site interfaces.

To gain insights into how the five different subunits assemble into a single pentameric L-AChR and how ACh and anthelmintic agents interact, we performed *in silico* studies using homology models of the extracellular domain of the L-AChR based on the nicotine-AChBP complex (PDB 1UW6). It should be taken into account that our model cannot provide any information about the role of Loop F in anthelmintic binding. Functional studies may be carried out to explore its role.
Out of the twenty four possible configurations for the arrangement of five different subunits, we tested four in which the three α-type subunits are non consecutive in the pentameric arrangement based on results from vertebrate AChRs (Rayes et al., 2009; Mazzaferro et al., 2011) and there is a glutamine at position 57 of the complementary face, which has been shown to be required for activation by anthelmintics (Bartos et al., 2006, 2009b; Martin et al., 2007) (Fig. 6).

Agonist binding sites in Arrangement 1 are located at UNC-38(+)/UNC-63(-), UNC-63(+)/LEV-1(-), and LEV-8(+)/UNC-29(-) interfaces (Fig. 6 and Supplemental Table 1). For the first two interfaces, ACh docking resulted in a main energetically favorable model with ACh oriented with its quaternary amine toward the membrane side or lower part of the cleft, similarly to carbamylcholine (CCh) in AChBP (Celie et al., 2004) (Binding energy ~-5 kcal/ mol). The positively charged group shows the potential to form the typical cation-π interaction with the indol group of W149 in Loop B (Fig. 6A,C and Supplemental Table 1). There is also the potential of ACh to interact with W55 in Loop D of the complementary face and to form additional H-bonds with A119 (UNC-38(+)/UNC-63(-) interface, Fig 6A) or V117 (UNC-63(+)/LEV-1(-), Fig. 6C) of Loop E. For the LEV-8(+)/UNC-29(-) a similar orientation of ACh is achieved in ~2% of the docking runs (Binding energy ~-4.8 kcal/mol. Fig. 6D) whereas in ~89% of the docking runs the agonist is positioned in opposite (upside down) orientation (Supplemental Fig. 4).

Protonated levamisole docks into the three interfaces (Fig. 6B-D). The molecule is oriented such that the imidazothiazole group is in the upper part of the cleft and the phenyl group is located

Molecular Pharmacology Fast Forward. Published on June 25, 2012 as DOI: 10.1124/mol.112.079962
This article has not been copyedited and formatted. The final version may differ from this version.

close to W55 (Binding energy ~ -7 kcal/mol). A cation-π interaction between the protonated nitrogen in the imidazothiazole group and W149 is possible (Supplemental Table 1). Only for the UNC-63(+)/LEV-1(-) interface, models with levamisole in opposite orientation were also obtained (Supplemental Fig. 4).

Because the pKa of levamisole is ~8 (Clarke, 1986) both protonated and non protonated forms co-exist at pH 7.4. Non protonated levamisole docks similarly into the UNC-38(+)/UNC-63(-), LEV-8(+)/UNC-29(-), and UNC-63(+)/LEV-1(-) interface. Interestingly, in all models the molecule is positioned opposite to its protonated form, with the imidazothiazole group oriented toward the membrane, and it cannot form cation-π interactions (Supplemental Fig. 4).

At UNC-63(+)/UNC-29(-) (Fig. 6E) and LEV-8(+)/LEV-1(-)interfaces (Fig. 6F) of Arrangement 2, ACh adopts the expected orientation with the potential to form the cation-π interaction with W149, interactions with Y190 and Y198, and a hydrogen bond with V117 (Loop E) (Fig. 6E,F). Protonated levamisole also docks into both interfaces with the imidazothiazole group oriented at the top of the cleft but without the potential to make a cation-π interaction with W149 (Figs. 6E,F) and with binding energies higher than for ACh (Supplemental Table 1).

In Arrangement 3, ACh docks into LEV-8(+)/UNC-63(-) and UNC-38(+)/LEV-1(-) interfaces with binding energies of ~-5 kcal/ mol and shows potential cation-π interactions with W149, Y190 or Y198 (Fig. 6G,H, Supplemental Table 1). At the minus face, the trimethylammonium group is close to W55 and the acetyl group, to A119 of UNC-63 or V117 of LEV-1. Thus, these two interfaces may be appropriate for channel activation. In both interfaces, protonated levamisole is orientated as in UNC-38(+)/UNC-63(-) (Fig. 6B and Supplemental Table 1).

In Arrangement 4, the UNC-38(+)/UNC-29(-) interface binds ACh (binding energy ~-5 kcal/mol) and protonated levamisole (binding energy ~-8.2 kcal/ mol) with the expected orientations (Fig. 6I, Supplemental Table 1).

Molecular Pharmacology Fast Forward. Published on June 25, 2012 as DOI: 10.1124/mol.112.079962
This article has not been copyedited and formatted. The final version may differ from this version.

Since our experimental results demonstrate that ACR-8 can replace LEV-8 in the pentameric arrangement, we docked ACh and protonated levamisole into binding site interfaces containing ACR-8 as a principal face and LEV-1, UNC-29 or UNC-63 as the complementary faces. For all interfaces, the orientation of ACh and protonated levamisole was similar to that found with LEV-8 as the principal face (Supplemental Fig. 5). ACh can form a cation-π interaction with W149 and H-bonds with V117 (of UNC-29 and LEV-1) or A119 (of UNC-63). Although these molecular docking results cannot explain the differences in the activation properties between wild-type and L-AChRs lacking LEV-8, such as increased desensitization and decreased levamisole sensitivity, they confirm that ACR-8 may provide a principal face with the capability of being activated by ACh and levamisole.

Molecular Pharmacology Fast Forward. Published on June 25, 2012 as DOI: 10.1124/mol.112.079962
This article has not been copyedited and formatted. The final version may differ from this version.

Discussion

This study provides experimental evidence of the subunit composition of L-AChR at larva1, its contribution to ACh-elicited responses, the role of LEV-8 subunit in the desensitization process, and the capability of ACR-8 subunit to replace LEV-8. We took advantage of a culture method in which embryonic cells differentiate into the cell types that comprise the L1 larva. Morphological, electrophysiological, and GFP reporter studies demonstrated that differentiation and functional properties of these cultured cells are similar to those observed *in vivo* (Christensen et al., 2002).

We have previously determined that UNC-38, UNC-63 and UNC-29 are essential while LEV-1 is not essential for functional expression of L-AChR in L1 muscle (Rayes et al., 2007). Here we show that LEV-8, an α-type subunit, is not essential for functional receptors but it is preferentially incorporated into native L-AChRs since its absence leads to kinetic changes. Single-channel activity of L-AChRs lacking LEV-8 decreases significantly with time and occurs in clusters, indicating that this subunit plays an important role as a determinant of desensitization. In addition, the duration of the open state is prolonged and the activation rate, faster in L-AChR lacking LEV-8. The functional changes do not affect significantly the motility of the adult worm. The absence of LEV-8, however, reduces levamisole sensitivity, which is evidenced at the single-channel level by the prolonged duration of closed periods, and at the worm level, by the partial resistance to the anthelmintic.

The lack of ACR-8 affects neither single L-AChR channel properties nor the phenotype, thus indicating this subunit is not part of the native L-AChR.

Taken together, the systematic analysis of single L-AChR-channel properties from null mutants for the six muscle L-AChR subunits indicate that five different subunits: UNC-63, UNC-38, UNC-29, LEV-1 and LEV-8 assemble into a single or at least a main functional form of L-AChR in L1 muscle (Fig. 7A). We have previously shown that the non-α type subunit, LEV-1, can

be replaced by another, not yet identified subunit, leading to L-AChRs with lower conductance (Fig. 7B, Rayes et al., 2007).

We asked if ACR-8, whose function remained unknown, could replace the close-related LEV-8 subunit. Our single-channel study in the double LEV-8/ACR-8 mutant confirmed that ACR-8 replaces LEV-8 in its absence (Fig. 7C). This is supported by the fact that in the absence of both subunits channel activity is not detected in most of the patches. Moreover, the active patches show opening events significantly briefer than those of wild-type and *lev-8* or *acr-8* single null mutants. Also, the frequency of opening events activated by levamisole is markedly reduced, indicating reduced sensitivity to the anthelmintic drug. Thus, LEV-8 and ACR-8 subunits may be replaced by another not yet identified subunit (Fig. 7D), leading to functional L-AChRs with very low expression and/or open probability and reduced levamisole sensitivity. These molecular changes are translated into important phenotypic changes, evidenced by uncoordinated locomotion probably due to reduced ACh responses and stronger resistance to the paralyzing effect of levamisole.

An alternative possibility is that the absence of both LEV-8 and ACR-8 completely abolishes function of L-AChRs but only in body muscle cells (as determined in 70% of the patches) instead of significantly decreasing expression and/or open probability in all muscle cells. This would indicate the presence of at least two different subset of muscle cells in the culture, which could be supported by the fact that in the single *lev-8* null mutant the body wall muscles but not the head muscles are contracted in the presence of levamisole. However, we did not detect heterogeneity in single-channel activity between different patches in wild-type and single LEV-8 null mutant, in contrast to what would be expected under the light of this possibility.

Interestingly, LEV-8 subunit has not been detected in Trichostrongylid parasites and ACR-8 is the candidate to replace it in L-AChRs (Fauvin et al., 2010; Neveu et al., 2010). Since this receptor constitutes the target of levamisole, ACR-8 may be involved in the molecular mechanisms

leading to levamisole-resistance acquisition. Thus, *lev-8* null mutants might be good models for studying anthelmintic drugs in these parasites.

Although the subunit composition of native wild-type L-AChR seems to be the same in L1 and adult muscle (Boulin et al., 2008; Qian et al., 2008), the relative contribution of L-AChR to the total ACh-activated current is different at both developmental stages. Our whole-cell recordings in L1 muscle cells show that at L1 the majority of the current is mediated by L-AChR. The contribution of N-AChR seems to be insignificant since only 25% of the cells show detectable currents, and when detected, currents are very small and decay rapidly. These results are in full agreement with the lack of detection of single N-AChR channels in cell-attached patches probably due to the fact that receptors desensitize during seal formation (Rayes et al., 2007). In contrast, the contribution of N-AChRs to ACh-activated responses is more significant in the adult (Touroutine et al., 2005; Almedom et al., 2009), revealing that although the subunit composition of both receptors is the same, their relative functional expression changes during development. The fact that levamisole sensitive function is crucial for the entire motor behavior of L1 worms but is only critical for forward behavior in the adult further supports this hypothesis (Lewis et al., 1980).

Macroscopic current recordings show that L-AChRs from wild-type L1 cells are capable of desensitizing, although more slower and to a less extent than N-AChRs. Whole-cell recordings in *Xenopus laevis* oocytes expressing L-AChRs show no desensitization (Boulin et al., 2008). This apparent controversy may be explained by the fact that accurate measurements of desensitization rates require optimal time-resolution systems, which is not the case for studies in oocytes (Bartos et al., 2009a). Our rapid perfusion system (Corradi et al., 2009) combined with the small size of the L1 muscle cells allow high temporal resolution. Also, desensitization could depend on the cellular environment (Hoffman et al., 1994) or on the expression of different regulatory proteins (Almedom et al., 2009).

Molecular Pharmacology Fast Forward. Published on June 25, 2012 as DOI: 10.1124/mol.112.079962
This article has not been copyedited and formatted. The final version may differ from this version.

We have used information available from the x-ray crystal structure of the water-soluble AChBP, which has emerged as a high-resolution model for the extracellular domain of Cys-loop receptors (Brejc et al., 2001) to model the ligand binding domain of L-AChR. Docking procedures reveal models for ACh binding into all binding-site interfaces with a similar orientation to that described for CCh in AChBP (Celie et al., 2004).

Residues close to ACh are the same as those described as part of the binding site in vertebrate AChRs, such as Y93, W149, Y190, Y198, the conserved double cysteine, and W55 (Rucktooa et al., 2009). A common feature for all binding models is the plausible interaction between the quaternary ammonium group of ACh and the indol group of W149, an interaction which has been shown to be required for high-efficacy activation (Xiu et al., 2009). Our studies also identify residues at Loop E of the complementary face that have the potential to form additional H-bonds with ACh and may be involved not only in its correct localization but also in channel gating. The models show that V117 in UNC-29 and LEV-1 and A119 in UNC-63 may form an H-bond with ACh in all tested interfaces. These residues are homologous to the functionally important residue, β2L119, of neuronal AChRs (Blum et al., 2010).

Levamisole docking supports the experimental findings revealing that this drug behaves as a potent but low-efficacy agonist of native wild-type L-AChRs at L1 stage. The high potency is evidenced by the lower levamisole concentration required for detecting single-channel activity and by the briefer closing periods in wild-type channels activated when compared to ACh. In agreement with this, docking studies reveal that levamisole binds with higher energy than ACh. The low efficacy is observed in whole-cell recordings from *acr-16* null mutants that show that current amplitudes activated by high levamisole concentrations are smaller than those activated by ACh in the same cell, in full agreement with results from heterologously expressed L-AChRs (Boulin et al., 2008). Protonated and non protonated forms of levamisole, which co-exist at pH 7.4, dock into the binding pocket in opposite orientations and only the protonated forms may make the typical cation-

Molecular Pharmacology Fast Forward. Published on June 25, 2012 as DOI: 10.1124/mol.112.079962
This article has not been copyedited and formatted. The final version may differ from this version.

π with W149 required for effective activation. Moreover, at some interfaces even protonated levamisole may not form this interaction. Thus, a possible explanation of levamisole not being as efficacious as ACh is that it can adopt multiple orientations at the binding site, as described before for other partial agonists (Hibbs et al., 2009).

These molecular modeling studies open doors for further experimental studies aiming at the identification of new determinants of anthelmintic selectivity and the discovery of how five different subunits are arranged in the pentameric L-AChR.

The combination of functional studies on mutant receptors with molecular docking studies is a powerful tool for the identification of determinants of anthelmintic selectivity and the elucidation of mechanisms of anthelmintic resistance. Also, the docking approach can be used to screen large compound libraries to select high affinity ligands that can be further experimentally tested.

Acknowledgments: We thank Dr. Mark Alkema for assistance in the generation of the double mutant.

Author Contribution:

Participated in research design: Hernando, Berge, Rayes, Bouzat.
Conducted experiments: Hernando, Berge, Rayes, Bouzat
Performed data analysis: Hernando, Berge, Rayes, Bouzat
Wrote or contributed to the writing of the manuscript: Hernando, Berge, Rayes, Bouzat

References

Almedom RB, Liewald JF, Hernando G, Schultheis C, Rayes D, Pan J, Schedletzky T, Hutter H, Bouzat C, and Gottschalk A (2009) An ER-resident membrane protein complex regulates nicotinic acetylcholine receptor subunit composition at the synapse. *EMBO J* **28**: 2636-2649.

Auerbach A, and Akk G (1998) Desensitization of mouse nicotinic acetylcholine receptor channels. A two-gate mechanism. *J Gen Physiol* **112**:181-197.

Bartos M, Rayes D, and Bouzat C (2006) Molecular determinants of pyrantel selectivity in nicotinic receptors. *Mol Pharmacol* **70:** 1307-1318

Bartos M, Corradi J, and Bouzat C (2009a) Structural basis of activation of Cys-Loop receptors: the extracellular-transmembrane interface as a coupling region. *Mol Neurobiol* **40**: 236-252

Bartos M, Price KL, Lummis SC, and Bouzat C (2009b) Glutamine 57 at the complementary binding site face is a key determinant of morantel selectivity for α7 nicotinic receptors. *J Biol Chem* **284**: 21478-21487

Blum AP, Lester HA, and Dougherty DA (2010) Nicotinic pharmacophore: The pyridine N of nicotine and carbonyl of acetylcholine hydrogen bond across a subunit interface to a backbone NH. *Proc. Natl. Acad. Sci. U S A.* **30**: 13206-13211

Boulin T, Gielen M, Richmond JE, Williams DC, Paoletti P, and Bessereau JL (2008) Eight genes are required for functional reconstitution of the *Caenorhabditis elegans* levamisole-sensitive acetylcholine receptor. *Proc Natl Acad Sci U S A* **105:** 18590-18595

Bouzat C (2012) New insights into the structural bases of activation of Cys-loop receptors. *J Physiol Paris* **106**:23-33.

Brejc K, van Dijk WJ, Klaassen RV, Schuurmans M, van Der Oost J, Smit AB, and Sixma TK (2001) Crystal structure of an ACh-binding protein reveals the ligand-binding domain of nicotinic receptors. *Nature* **411:** 269-276

Brown LA, Jones AK, Buckingham SD, Mee CJ, and Sattelle DB (2006) Contributions from *Caenorhabditis elegans* functional genetics to antiparasitic drug target identification and validation: nicotinic acetylcholine receptors, a case study. *Int J Parasitol* **36:** 617-624

Celie PH, van Rossum-Fikkert SE, van Dijk WJ, Brejc K, Smit AB, and Sixma TK (2004) Nicotine and carbamylcholine binding to nicotinic acetylcholine receptors as studied in AChBP crystal structures. *Neuron* **41:** 907-14

Christensen M, Estevez A, Yin X, Fox R, Morrison R, McDonnell M, Gleason C, Miller DM 3rd, and Strange K (2002) A primary culture system for functional analysis of *C. elegans* neurons and muscle cells. *Neuron* **33:** 503-514

Clarke EGC (1986) Clarke's Isolation and Identification of Drugs in pharmaceuticals body fluids and post-mortem material (Moffat, AC, ed) 2nd edition, Pharmaceutical Press, London.

Corradi J, Gumilar F, and Bouzat C (2009) Single-channel kinetic analysis for activation and desensitization of homomeric 5-HT(3)A receptors. *Biophys J* **97:** 1335-1345

Culetto E, Baylis HA, Richmond JE, Jones AK, Fleming JT, Squire MD, Lewis JA, and Sattelle DB (2004) The *Caenorhabditis elegans unc-63* gene encodes a levamisole-sensitive nicotinic acetylcholine receptor α subunit. *J Biol Chem* **279:** 42476-42483

Dilger JP, and Liu Y (1992) Desensitization of acetylcholine receptors in BC3H-1 cells. *Pflugers Arch* **420**:479-485.

Fauvin A, Charvet C, Issouf M, Cortet J, Cabaret J, Neveu C (2010) cDNA-AFLP analysis in levamisole-resistant *Haemonchus contortus* reveals alternative splicing in a nicotinic acetylcholine receptor subunit. *Mol Biochem Parasitol* **170**:105-107

Fire A, Xu S, Montgomery MK, Kostas SA, Driver SE, and Mello CC (1998) Potent and specific genetic interference by double-stranded RNA in *Caenorhabditis elegans*. *Nature* **391**: 806-811

Fleming JT, Squire MD, Barnes TM, Tornoe C, Matsuda K, Ahnn J, Fire A, Sulston JE, Barnard EA, Sattelle DB and Lewis JA (1997) *Caenorhabditis elegans* levamisole resistance genes lev-1, unc-29, and unc-38 encode functional nicotinic acetylcholine receptor subunits. *J Neurosc* **17:** 5843-5857

Francis MM, Evans SP, Jensen M, Madsen DM, Mancuso J, Norman KR, and Maricq AV (2005) The Ror receptor tyrosine kinase CAM-1 is required for ACR-16-mediated synaptic transmission at the *C. elegans* neuromuscular junction. *Neuron* **46:** 581-594

Gottschalk A, Almedom RB, Schedletzky T, Anderson SD, Yates JR 3rd, and Schafer WR (2005) Identification and characterization of novel nicotinic receptor-associated proteins in *Caenorhabditis elegans*. *EMBO J* **24**: 2566-2578

Gumilar F, Arias HR, Spitzmaul G, and Bouzat C (2003) Molecular mechanisms of inhibition of nicotinic acetylcholine receptors by tricyclic antidepressants. *Neuropharmacol* **45:** 964-976.

Hall ZW, and Sanes JR (1993) Synaptic structure and development: the neuromuscular junction. *Cell* **72**:99-121.

Hibbs RE, Sulzenbacher G, Shi J, Talley TT, Conrod S, Kem WR, Taylor P, Marchot P, and Bourne Y (2009) Structural determinants for interaction of partial agonists with acetylcholine binding protein and neuronal alpha7 nicotinic acetylcholine receptor *EMBO J*. **28:** 3040-3051

Hoffman PW, Ravindran A, and Huganir RL (1994) Role of phosphorylation in desensitization of acetylcholine receptors expressed in *Xenopus* oocytes. *J Neurosci* **14:** 4185-4195

Jones AK, Buckingham SD, and Sattelle DB (2005) Chemistry-to-gene screens in *Caenorhabditis elegans*. *Nat Rev Drug Discov* **4:** 321-330

Jones AK, Rayes D, Al-Diwani A, Maynard TP, Jones R, Hernando G, Buckingham SD, Bouzat C, and Sattelle DB (2011) A Cys-loop mutation in the *Caenorhabditis elegans* nicotinic receptor subunit UNC-63 impairs but does not abolish channel function. *J Biol Chem* **286:** 2550-2558

Lewis JA, Wu CH, Berg H, and Levine JH (1980) The genetics of levamisole resistance in the nematode *Caenorhabditis elegans*. *Genetics* **95**: 905-928

Martin RJ, and Robertson AP (2007) Mode of action of levamisole and pyrantel, anthelmintic resistance, E153 and Q57. *Parasitol* **134**: 1093-1104

Mazzaferro S, Benallegue N, Carbone A, Gasparri F, Vijayan R, Biggin PC, Moroni M, and Bermudez I (2011) Additional Acetylcholine (ACh) Binding Site at α4/α4 Interface of (α4β2)2α4 Nicotinic Receptor Influences Agonist Sensitivity. *J Biol Chem* **286**: 31043-31054

Mongan NP, Baylis HA, Adcock C, Smith GR, Sansom MS, and Sattelle DB (1998) An extensive and diverse gene family of nicotinic acetylcholine receptor alpha subunits in *Caenorhabditis elegans*. *Receptors Channels* **6:** 213-228

Mongan NP, Jones AK, Smith GR, Sansom MS, and Sattelle DB (2002) Novel alpha7-like nicotinic acetylcholine receptor subunits in the nematode *Caenorhabditis elegans*. *Protein Sci* **11:** 1162-1171

Morris G, Goodsell DS, Halliday RS, Huey R, Hart WE, Belew RK, and Olson AJ (1998) Automated docking using a Lamarckian genetic algorithm and empirical binding free energy function. *J Comput Chem* **19:** 1639-1662.

Neveu C, Charvet CL, Fauvin A, Cortet J, Beech RN, and Cabaret J (2010) Genetic diversity of levamisole receptor subunits in parasitic nematode species and abbreviated transcripts associated with resistance. *Pharmacogenet Genomics* **20**: 414-425.

Qian H, Robertson AP, Powell-Coffman JA, and Martin RJ (2008) Levamisole resistance resolved at the single-channel level in *Caenorhabditis elegans*. *FASEB J* **22**: 3247-3254

Rand JB (2007) Acetylcholine. In *WormBook* ed. The *C. elegans* Research Community, WormBook, doi/10.1895/wormbook. 1.131.1, http://www.wormbook.org.

Rayes D, De Rosa MJ, Bartos M and Bouzat C (2004) Molecular basis of the differential sensitivity of nematode and mammalian muscle to the anthelminitic agent levamisole. *J. Biol. Chem*. **279**:36372-36381.

Rayes D, Flamini M, Hernando G, and Bouzat C (2007) Activation of single nicotinic receptor channels from *Caenorhabditis elegans* muscle. *Mol Pharmacol* **71**: 1407-1415

Rayes D, De Rosa MJ, Sine SM, and Bouzat C (2009) Number and locations of agonist binding sites required to activate homomeric Cys-loop receptors. *J Neurosci* **29**: 6022-6032

Reeves DC, Sayed MF, Chau PL, Price KL, and Lummis SC (2003) Prediction of 5-HT3 receptor agonist-binding residues using homology modeling. *Biophys J* **84:** 2338-2344

Richmond JE, and Jorgensen EM (1999) One GABA and two acetylcholine receptors function at the *C. elegans* neuromuscular junction. *Nat Neurosci* **2:** 791-797

Rucktooa P, Smit AB, and Sixma TK (2009) Insight in nAChR subtype selectivity from AChBP crystal structures. *Biochem Pharmacol* **78:** 777-787

Salamone FN, Zhou M, and Auerbach A (1999) A re-examination of adult mouse nicotinic acetylcholine receptor channel activation kinetics. *J Physiol* **516:**315-330

Sali A, Potterton L, Yuan F, van Vlijmen H, and Karplus M (1995) Evaluation of comparative protein modeling by MODELLER. *Proteins* **23:** 318-326

Taly A, Corringer PJ Guedin D, Lestage P and Changeux JP (2009) Nicotinic receptors: allosteric transitions and therapeutic targets in the nervous system. *Nat Rev Drug Discov* **8:** 733-750

Touroutine D, Fox RM, Von Stetina SE, Burdina A, Miller DM 3rd, and Richmond JE (2005) acr-16 encodes an essential subunit of the levamisole-resistant nicotinic receptor at the *Caenorhabditis elegans* neuromuscular junction. *J Biol Chem* **280:** 27013-27021

Towers PR, Edwards B, Richmond JE, and Sattelle DB (2005) The *Caenorhabditis elegans lev-8* gene encodes a novel type of nicotinic acetylcholine receptor alpha subunit. *J Neurochem* **93:** 1-9

Unwin N (2005) Refined structure of the nicotinic acetylcholine receptor at 4A resolution. *J Mol Biol* **346**: 967-989

Xiu X, Puskar NL, Shanata JA, Lester HA, and Dougherty DA (2009) Nicotine binding to brain receptors requires a strong cation-pi interaction. *Nature* **458**: 534-537

Footnotes

a) **Financial Support:** Supported by Universidad Nacional del Sur (UNS), Agencia Nacional de Promoción Científica y Tecnológica (ANPCYT), and Consejo Nacional de Investigaciones Científicas y Técnicas (CONICET).

b) **This study has been presented in** 40th annual meeting of Society for Neuroscience. San Diego, CA. U.S.A. Noviembre 2010 Poster 38.16/F30. Hernando, G., Rayes, D. and Bouzat C. "Contribution of LEV-8 subunit to the kinetics of activation and desensitization of *C. elegans* muscle levamisole-sensitive nicotinic receptors".

c) **Correspondence author**: Cecilia Bouzat- Instituto de Investigaciones Bioquimicas- Camino La Carrindanga Km 7- 8000 Bahía Blanca- Argentina. FAX: 54-291-4861200. E-mail: inbouzat@criba.edu.ar.

Molecular Pharmacology Fast Forward. Published on June 25, 2012 as DOI: 10.1124/mol.112.079962
This article has not been copyedited and formatted. The final version may differ from this version.

Figure Legends

Figure 1- Behavioral and molecular changes in worms lacking LEV-8 or/and ACR-8 subunits. A)Left: Thrashing rate of wild-type (N2) and mutant worms in M9 solution. Right: Fraction of moving animals as a function of time on 0.2 mM levamisole. Data are plotted as mean ± SD. One-way ANOVA with Bonferroni's multiple comparison post test: * $p< 0.05$; ** $p< 0.01$; *** $p<0.001$. B) Single-channel recordings from cultured muscle cells derived from wild type (N2 Bristol), *lev-8(x15)*, *acr-8 (ok1240)*, and *lev-8(ok1519); acr-8 (ok1240)* strains in the presence of 1 µM ACh (Left) or levamisole (Right). Membrane potential: -100 mV. Channel openings are shown as upward deflections and traces are shown at two different time scales. Filter: 9 kHz. Representative open time histograms are shown for each strain. The durations of the open components and relative areas (in brackets) are: 1 µM ACh: wild-type: 0.28 ms (0.87) and 0.46 ms (0.12); *lev-8(x15)*: 0.40 ms (0.9) and 0.90 ms (0.1); *acr-8 (ok1240)*: 0.23 ms (0.86) and 0.35 ms (0.13); and *lev-8(ok1519); acr-8 (ok1240)*: 0.23 ms (1). For 1 µM levamisole: wild-type: 0.33 ms (1); *lev-8(x15)*: 0.30 ms (0.9) and 0.85 ms (0.1); *acr-8 (ok1240)*: 0.26 ms (1); and *lev-8(ok1519); acr-8 (ok1240)*: 0.22 ms (1). The mean values of the components are shown in Table 1.

Figure 2- L-AChR channel currents at different potentials. Single-channel recordings were obtained from cultured muscle cells of *lev-8(x15)* mutants. ACh concentration: 1 µM. Left: Traces of single-channel activity at the indicated membrane potential are shown filtered at 9 kHz with channel openings as upward deflections. Middle: Representative amplitude histograms for each condition are shown. Mean amplitudes of the shown histograms are: 2.36 pA (-70 mV), 3.47 pA (-100 mV), 4.31 pA (-120 mV). The mean values (± SD) of the amplitudes at each potential are: 2.35 ± 0.13 pA (-70 mV), 3.5 ± 0.27 pA (-100 mV), 4.3 ± 0.28 pA (-120 mV), n=7. Right: Current-voltage relationships for wild type (□); *lev-8(x15)* (▲); *acr-8(ok1240)* (●); and *lev-8(ok1519); acr-8(ok1240)* (○).

Molecular Pharmacology Fast Forward. Published on June 25, 2012 as DOI: 10.1124/mol.112.079962
This article has not been copyedited and formatted. The final version may differ from this version.

Figure 3- Activation of L-AChRs lacking LEV-8 as a function of agonist concentration. AChR channels were recorded from cultured muscle cells of *lev-8(x15*) at different ACh (A) or levamisole (B) concentrations. Filter: 9 kHz. Membrane potential: -100 mV. Representative open and closed duration histograms are shown. Mean duration of the components are: 1 μM ACh: Open: 0.40 ms (0.90) and 0.84 ms (0.10); Closed: 0.06 ms (0.11), 150 ms (0.87), and 991 ms (0.01). 100 μM ACh: Open: 0.37 ms (1); Closed: 0.064 ms (0.64), 20 ms (0.27), 73 ms (0.07), and 4070 ms (0.008). 300 μM ACh: Open: 0.16 ms (1); Closed: 0.048 ms (0.31), 7.6 ms (0.65), 26 ms (0.03), and 9181 ms (0.005). 0.1 μM levamisole: Open: 0.27 ms (0.88) and 0.80 ms (0.12); Closed: 0.17 ms (0.10), 1.7 ms (0.10), and 580 ms (0.85). 50 μM levamisole: Open: 0.28 ms (1); Closed: 0.08 ms (0.20), 1.30 ms (0.07), 100 ms (0.70), and 5600 ms (0.017). 100 μM levamisole: Open: 0.24 ms (1); Closed: 0.08 ms (0.09), 2.5 ms (0.22), 16 (0.66) and 227 ms (0.04). The mean values of the open components are shown in Table 1.

Figure 4- Single-channel activity of L-AChRs lacking LEV-8 decreases significantly with time and occurs in clusters. A. *Left:* Continuous recordings from muscle cells derived from wild type and *lev-8(x15)* mutant at 100 μM ACh or levamisole. Membrane potential: -100 mV. Filter: 9 kHz. *Right:* Percentage of opening events per minute during the 7 min-recording. B. Typical clusters of L-AChR lacking LEV-8 at 100 and 300 μM ACh.

Figure 5- Macroscopic current recordings reveal increased desensitization of L-AChRs lacking LEV-8. A) Whole-cell currents from cultured muscle cells of wild-type and *lev-8(x15)* mutants elicited by a 2 s-pulse of 500 μM ACh (black) or 500 μM levamisole (grey). B) ACh-elicited currents from cultured muscle cells of *acr-16* (*acr-16(ok789*)) and *unc-29* (*unc-29(e1072)*) null mutant strains. c) Peak current (%) respect to wild-type cells. ***p<0.001 Student *t*-test. Pipette potential: -70 mV.

Figure 6- Docking of ACh and anthelmintic agents into homology-modeled L-AChR binding-site interfaces. The four tested arrangements (1-4) are shown in the left with the arrows at potential binding sites. Top panel: Docking of ACh (A) and protonated levamisole (B) into UNC-38(+)/UNC-63(-) interface. Panels c-i correspond to docking of ACh (top) and levamisole (bottom) into the specified interfaces. Binding loops and their corresponding residues are colored yellow (Loop A), cyan (Loop B), red (Loop C), green (loop D) and blue (loop E). Agonists are shown in grey with the atoms colored as follows: N in violet, O in red, S in yellow, H+ in light grey. In the minus face provided by LEV-1 and UNC-29 subunits, the equivalent residue to A119 UNC-63 is V117.

Figure 7- Schemes of functional L-AChRs in larval musle. The disposition of the subunits in the pentamer has not yet been determined. Subunits not yet identified are shown in grey. A. Subunit composition in L1 muscle of wild-type worms. B. Functional L-AChRs are observed in the absence of *lev-1* (Rayes et al., 2007). C. LEV-8 can be replaced by ACR-8. D. LEV-8 can be replaced by other, not yet identified, subunit in the LEV-8/ACR-8 double null mutant.

Molecular Pharmacology Fast Forward. Published on June 25, 2012 as DOI: 10.1124/mol.112.079962
This article has not been copyedited and formatted. The final version may differ from this version.

Table 1. Single-channel properties of L-AChRs from wild-type and null mutant strains.

Agonist		wild-type			*lev-8(x15)*			*acr-8(ok1240)*			*lev-8(ok1519); acr-8(ok1240)*		
	µM	**O1 (ms) (area)**	**O2 (ms) (area)**	**n**	**O1 (ms) (area)**	**O2 (ms) (area)**	**n**	**O1 (ms) (area)**	**O2 (ms) (area)**	**n**	**O1 (ms) (area)**	**O2 (ms) (area)**	**n**
ACh	0.1	0.23±0.06 (0.81)	0.49±0.1 (0.19)	6	0.37±0.08 (0.81)	1.1±0.05 (0.19)	5	nm	nm		nm	nm	
	1	0.27±0.06 (0.83)	0.53±0.1 (0.17)	7	0.42±0.12 (0.74)	1.2±0.5 (0.25)	7	0.26±0.06 (0.86)	0.44±0.1 (0.13)	7	0.28±0.08 (1)	nd	7
	50	0.24±0.03 (0.88)	0.43 0.06 (0.12)	4	0.32 ±0.05 (0.84)	0.7 ±0.12 (0.16)	7	nm	nm		0.32 ±0.09 (1)	nd	4
	100	0.21±0.04 (1)	nd	8	0.33±0.05 (1)	nd	5	0.24±0.04 (1)	nd	3	0.19±0.05 (1)	nd	8
	300	0.14±0.02 (1)	nd	4	0.18±0.02 (1)	nd	4	nm	nm		nm	nm	
Lev	0.1	0.18±0.02 (0.85)	0.44±0.12 (0.15)	8	0.33±0.06 (0.86)	0.80±0.11 (0.14)	6	nm	nm		nm	nm	
	1	0.24±0.05 (1)	nd	6	0.40±0.13 (0.79)	0.98±0.09 (0.21)	4	0.29±0.06 (1)	nd	7	0.26±0.06 (1)	nd	6
	100	0.27±0.04 (1)	nd	4	0.21±0.03 (1)	nd	5	0.27±0.04 (1)	nd	3	0.16±0.07 (1)	nd	11

Single-channel recordings from muscle cultured cells of different strains were performed at a membrane potential of -100 mV in the presence of different ACh or levamisole concentrations. O1 and O2 correspond to the open components obtained from open time histograms with their relative

Molecular Pharmacology Fast Forward. Published on June 25, 2012 as DOI: 10.1124/mol.112.079962
This article has not been copyedited and formatted. The final version may differ from this version.

areas shown in brackets. n: number of recordings for each condition. nm: not measured. nd: not detected.

Figure 1

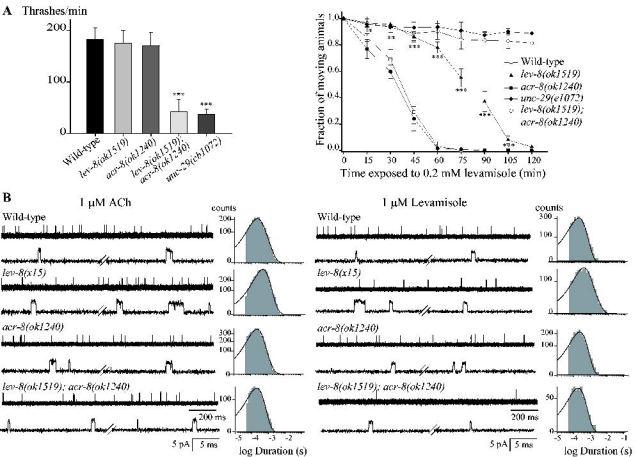
A
Thrashes/min
200
100
0
***
***
Wild-type
lev-8(ok1519)
acr-8(ok1240)
lev-8(ok1519); acr-8(ok1240)
unc-29(e1072)
Fraction of moving animals
1.0
0.8
0.6
0.4
0.2
0.0
0
15
30
45
60
75
90
105
120
Time exposed to 0.2 mM levamisole (min)
Wild-type
lev-8(ok1519)
acr-8(ok1240)
unc-29(e1072)
lev-8(ok1519); acr-8(ok1240)
B
1 µM ACh
1 µM Levamisole
Wild-type
lev-8(x15)
acr-8(ok1240)
lev-8(ok1519); acr-8(ok1240)
counts
200 ms
5 pA
5 ms
log Duration (s)
-5
-4
-3
-2
-1

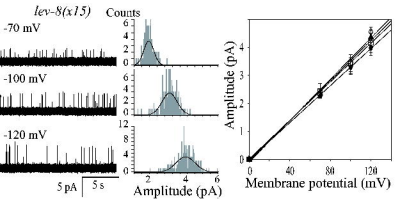
lev-8(x15)
Counts
-70 mV
-100 mV
-120 mV
5 pA
5 s
Amplitude (pA)
Amplitude (pA)
Membrane potential (mV)

Figure 2

Figure 3

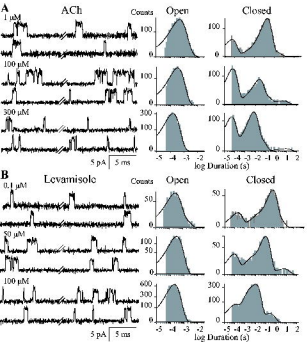
A
ACh
Counts
Open
Closed
1 μM
100 μM
500 μM
5 pA
5 ms
log Duration (s)
B
Levamisole
0.1 μM
50 μM
100 μM
5 pA
5 ms
log Duration (s)

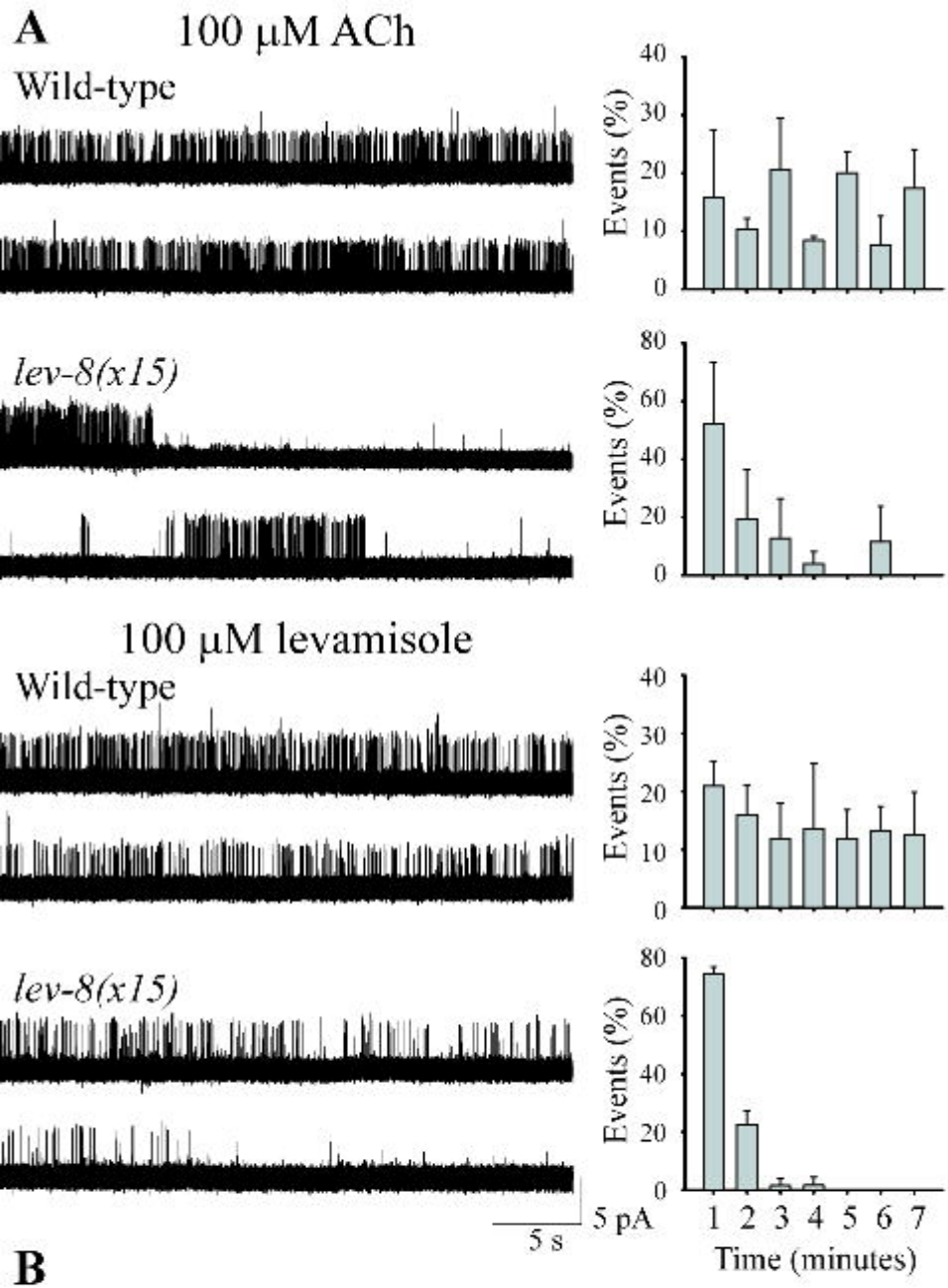
A
100 μM ACh
Wild-type
lev-8(x15)
Events (%)
100 μM levamisole
Wild-type
lev-8(x15)
Events (%)
5 pA
5 s
1 2 3 4 5 6 7
Time (minutes)

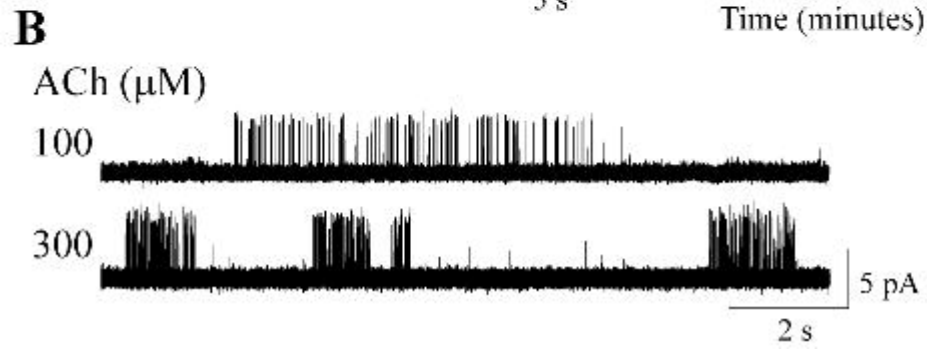
B
ACh (μM)
100
300
5 pA
2 s

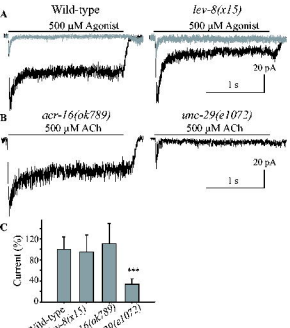
A
Wild-type
500 μM Agonist
lev-8(x15)
500 μM Agonist
20 pA
1 s
B
acr-16(ok789)
500 μM ACh
unc-29(e1072)
500 μM ACh
20 pA
1 s
C
Current (%)
120
80
40
0
***
Wild-type
lev-8(x15)
acr-16(ok789)
unc-29(e1072)

Figure 5

Figure 6

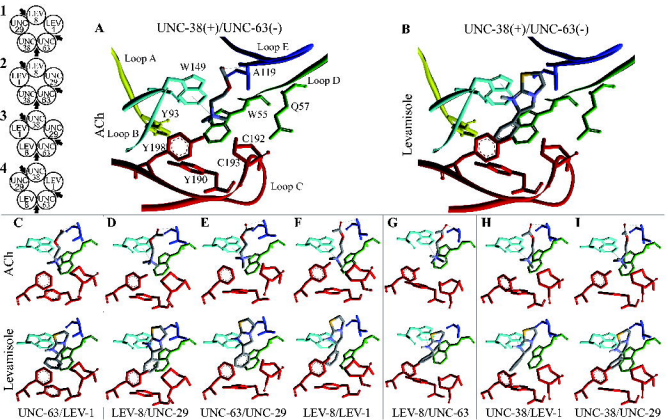
1
2
3
4
A
UNC-38(+)/UNC-63(-)
Loop A
W149
A119
Loop E
Loop D
Q57
W55
Y93
ACh
Loop B
Y198
C192
C193
Y190
Loop C
B
UNC-38(+)/UNC-63(-)
Levamisole
C
D
E
F
G
H
I
ACh
Levamisole
UNC-63/LEV-1
LEV-8/UNC-29
UNC-63/UNC-29
LEV-8/LEV-1
LEV-8/UNC-63
UNC-38/LEV-1
UNC-38/UNC-29

Figure 7

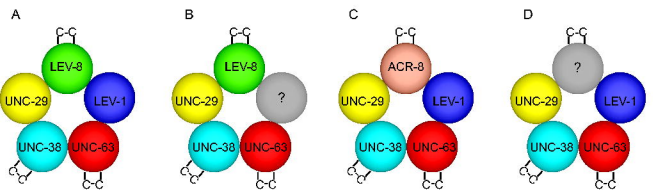
A
C-C
LEV-8
UNC-29
LEV-1
UNC-38
UNC-63
C-C
B
C-C
LEV-8
UNC-29
?
UNC-38
UNC-63
C-C
C
C-C
ACR-8
UNC-29
LEV-1
UNC-38
UNC-63
C-C
D
C-C
?
UNC-29
LEV-1
UNC-38
UNC-63
C-C